The Economically Sustainable Hydrothermal Synthesis of Dextrosil-Viologen as a Robust Anolyte in Aqueous Redox Flow Batteries

Xiu-Liang Lv[a†], Patrick Sullivan[b†], Hui-Chun Fu[b], XuanXin Hu[b], Honghao Liu[b], Song Jin[b], Wenjie Li[b*], and Dawei Feng[ab*]

[a] Department of Materials Science and Engineering, University of Wisconsin-Madison, Madison, Wisconisn, USA

[b] Department of Chemistry, University of Wisconsin-Madison, Madison, Wisconsin, USA

† These authors contributed equally to this work

* Corresponding authors: wli@chem.wisc.edu, dfeng23@wisc.edu

Abstract

Aqueous organic redox flow batteries (RFBs) are promising for grid-scale energy storage, but identifying stable and inexpensive organic redox couples suitable for practical applications has been challenging. Here we report a new, inexpensive, and robust anolyte, Dextrosil-Viologen (Dex-Vi), that demonstrates a record overall RFB performance for anolyte redox species in neutral aqueous media, including ultralow anion-exchange membrane permeability, high volumetric capacity capability, and outstanding chemical stability. Remarkably, at a high concentration of 1.5 M (40.2 Ah·L^{-1} theoretical anolyte volumetric capacity), Dex-Vi shows extremely stable cycling performance without observable capacity decay over one-month cycling. Furthermore, by rationalizing a high-yield hydrothermal synthetic approach that has never been applied to viologen

RFB molecules along with a low-cost precursor, the predicted mass production cost of Dex-Vi is below $10/kAh. These results not only establish a new benchmark organic anolyte promising for practical RFB applications but also shows that the properties of organic redox species can be enhanced with minute performance tradeoffs through rationalized structural and synthetic design.

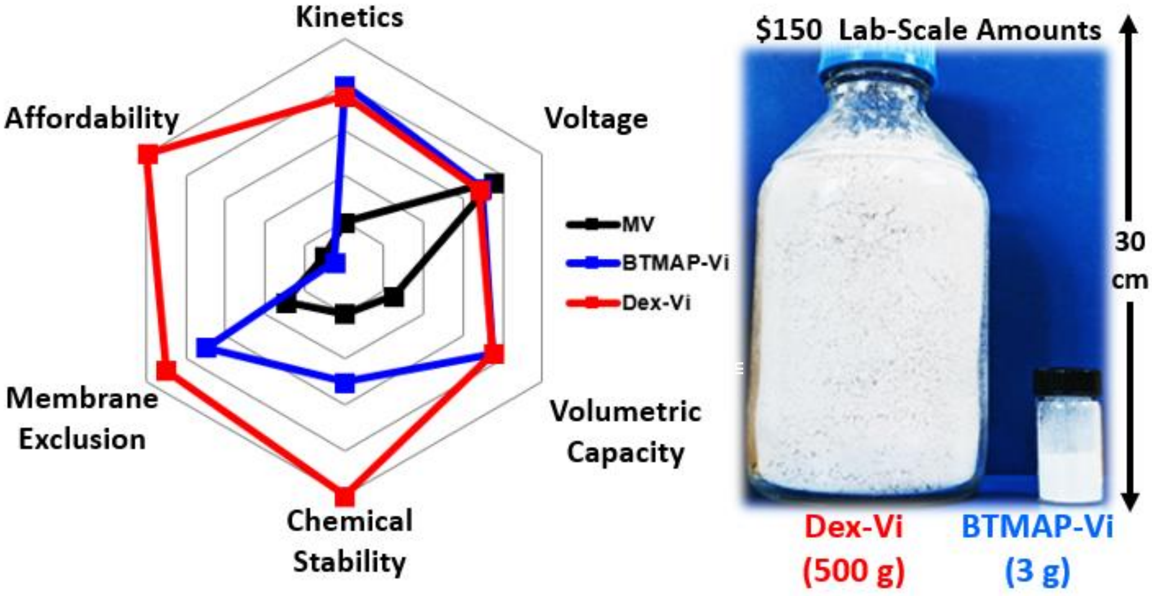

Introduction

As an increasing amount of renewable energy sources are being integrated into the electric grid in the US and around the world, low-cost grid-scale energy storage technology must be developed to balance the mismatched energy production and demand due to the intermittency of wind and solar energy resource. To date, Lithium-ion batteries have received the most attention, but they are less scalable and have short storage duration (power-energy ratio). This is in addition to the uncertain resource cost and availability of key raw materials for Lithium-ion anodes and cathodes.[1]

An alternative and promising approach to grid energy storage technology are redox flow batteries (RFBs), which have decoupled energy and power units that allows for simplified scaling of long storage duration devices.[2–11] Despite this advantage, RFBs have only been commercially implemented in a handful of experimental grid applications. This is partially due to the high and volatile cost of active materials in the most commercially mature vanadium RFBs. Aqueous Organic Redox Flow Batteries (AORFBs) are a promising approach to utilizing the scalability of liquid-state energy storage while reducing the materials cost using inexpensive organic redox molecules.[2–11] Furthermore, the extensive tunability of organic chemistry can be leveraged when there is a mechanistic understanding of the underlying physical, chemical, and electrochemical properties of the organic redox species. However, developing organic redox active species that are simultaneously aqueous soluble, chemically stable, high voltage, membrane compatible, and cost effective remains difficult.

Among the plethora of aqueous organic redox species, bis(3-trimethylammonio)propyl viologen tetrachloride (BTMAP-Vi), reported by Beh et al. in 2017,[12] has stood out as a promising aqueous anolyte. The presence of the trimethyl ammonium groups on the viologen core results in high water solubility, anion-exchange membrane compatibility, and excellent stability in neutral aqueous solution, making BTMAP-Vi the best performing anolyte among viologen derivatives.[13–17] Although BTMAP-Vi consists of earth-abundant atoms, the current synthetic procedure poses serious sustainability and cost concerns. The original synthetic procedure requires uncommon 1-bromo-3-chloropropane and trimethyl amine starting materials in excess to drive the reaction forward (Figure 1A), large amounts of expensive organic solvents (DMF, methyl tert-butyl ether, and isopropanol) to obtain pure product, and an ion-exchange step of the bromide counter-anion for chloride, but only produced a low overall yield of 44%.[12] This procedure was simplified by removing the need for the ion-exchange step, but an even more expensive starting material, 1,3-dicholorpropane, was used and the overall synthesis yield was reduced to 13%.[16] It has been demonstrated the synthesis of the tetrabromide salt of BTMAP-Vi has a relatively high yield of 68% in a single-step reaction.[15] However, using bromide as the counter ion for positively charged viologen derivatives suffers from several disadvantages. Firstly, the bromine/bromide redox couple has a formal potential of 1.09 V, which may interfere with high potential cathodic reactions in RFBs.[18] Secondly, bromide has lower conductivity than chloride through commonly used anion exchange membranes (AEMs) for positively charged viologen derivatives, resulting in diminished power. Finally, bromide salt form of viologen derivatives have lower aqueous solubility, higher viscosity, and increased mass, reducing both volumetric and gravimetric energy density. Thus, the chloride salts of viologen derivatives are more desirable for practical aqueous RFBs.

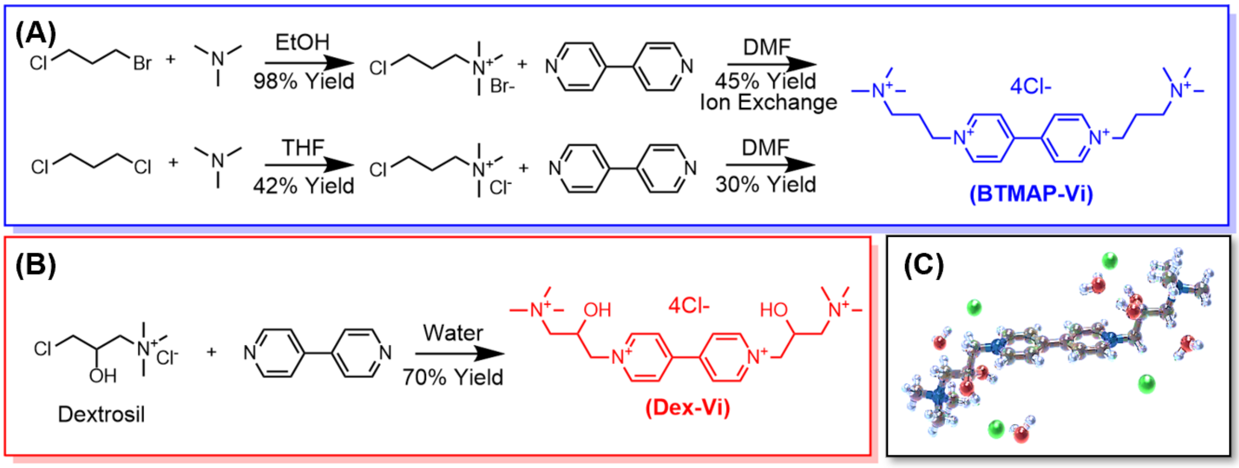

Figure 1. Comparison of the synthetic procedures of (A) BTMAP-Vi (blue) reported previously in literature[12,16] and our new (B) Dex-Vi (red) described in this report. (C) The experimentally determined single crystal structure of Dex-Vi (carbon is grey, nitrogen is blue, hydrogen is white, oxygen is red, and chloride is green).

Simply claiming all organic redox active species are inherently environmentally and economically sustainable alternatives to metal-based redox species could be misleading when the redox molecules are synthesized using expensive precursors and complex procedures with low yields.[19,20] This will become especially concerning when AORFBs are scaled up for Megawatt-hour to Gigawatt-hour, long-duration energy storage applications where large quantities of active materials must be used and will constitute a major portion of cost per capacity.[19] Herein, we report a truly sustainable and robust viologen redox species, namely bis(3-trimethylammonio-2-hydroxy)propyl viologen tetrachloride (Dex-Vi), synthesized from a common and inexpensive industrial chemical, 3-chloro-2-hydroxypropyl trimethylammonium chloride (commonly known as Dextrosil) (Figure 1B).[21] Dex-Vi exhibits a similar formal potential to BTMAP-Vi but with improved cycling stability and reduced membrane permeability in neutral aqueous solution. Dex-Vi shows very stable RFB cycling performance at high concentration (1.5 M) when paired with a stable bis(3-trimethylammonio)propyl ferrocene dichloride (BTMAP-Fc) catholyte. Produced from a simple and efficient synthetic procedure with readily available precursors possessing existing bulk-quantity supply chains, Dex-Vi is an ideal anolyte to enable AORFBs for practical grid-scale storage and facilitate the integration of renewable electricity generation technologies.

Results

Viologen derivatives are typically synthesized by alkylation of pyridine species in organic solvents.[12,15–17,22] Upon formation of the pyridinium containing species, the products always carry more charge than the starting materials, forming precipitates in the organic solutions for facile separation and purification. However, such synthetic routes become less efficient for producing the desired chloride containing viologens due to two major reasons. Firstly, the low activity of chloro- species often causes low yields for the S_N2 reaction as chlorine is the least facile leaving group of the halogens. Secondly, chloride-containing salts exhibit very poor solubility in organic solvents even at high temperature, which is problematic for the synthesis of bis-substituted viologen species as the asymmetric, mono-substituted bipyridine will precipitate out before the second pyridyl site reacts. The issue of forming mono-substituted byproduct becomes even more significant when the reactants already carry charge, which is often the case to achieve higher solubility in water for AORFBs (i.e. trimethylammonium or sulfate groups).[13–17,23–26] Such intrinsic synthetic complications often result in complex procedures and low yields, hindering the cost reduction even if the syntheses are scaled up.

To develop more cost-effective synthetic routes towards highly charged viologens, we identified Dextrosil as an alternative starting material. Dextrosil is an extremely inexpensive chemical that is widely used in various industrial processes, such as starch treatment, paper and textile manufacturing, and surfactant development.[21,27] The chloro- group in Dextrosil can react with the pyridyl site on 4,4'-bipyridine (Figure 1B) to yield the desired viologen product with a quaternary ammonium group that increases the product solubility in aqueous solution. Dex-Vi exhibits similar structure to BTMAP-Vi but with two additional hydroxyl groups which can presumably further improve its aqueous solubility. However, Dextrosil is fairly insoluble in organic solvents, so if the reaction is performed in organic solution, the mono-substituted bipyridine intermediate will immediately crash out of solution before complete reaction. Therefore, water is used as the reaction solvent to address this "solubility issue" because the starting materials, the intermediate, and the product are all highly aqueous soluble. Furthermore, to compensate the low reactivity of chloro- group of Dextrosil for S_N2 reaction, the reaction temperature is elevated to above the boiling point of water in autoclave reactors using a standard, simple hydrothermal reaction procedure.[28]

NMR and X-ray structural analysis (Figures. S1 & S2) confirmed the pure redox active Dex-Vi product was successfully obtained through the hydrothermal reaction. Single crystal X-ray structure solution shows the coordination of four water molecules and four chlorides to the

Dex-Vi molecule (Figure 1C), resulting in a molecular weight of 604 g·mol^{-1} ($C_{22}H_{38}O_2N_4Cl_4 \cdot 4H_2O$). This pure product was obtained in a high yield of 71% in small-batch and 70% yield in large-batch (> 600 g of product) synthesis (Figure S3). This high yield is expected considering the simplicity of the single-step reaction (Figure 1B). Additionally, the reaction does not use organic solvent, and the product purification requires only inexpensive organic solvents (i.e., ethanol and acetone). This is remarkable considering the synthesis of BTMAP-Vi requires expensive starting materials and solvents in large excess with multiple reaction and purification steps (Figure 1A), including an ion-exchange step to obtain the chloride salt which is difficult to scale up.[12,15–17,22] In contrast, through the use of Dextrosil, the chloride salt form of Dex-Vi is obtained directly, which is essential to maximizing the conductivity of anion-exchange membranes and for optimized volumetric and gravimetric energy densities. The performance of the Dex-Vi and BTMAP-Vi redox couples was compared through physical, electrochemical, and cycling experiments.

The solubility of a redox species typically determines the volumetric capacity of the flow battery. A maximum solubility of 1.7 M was obtained for Dex-Vi in pure water at room temperature (~18 ^oC), which is near the literature reported value of 2.0 M for BTAMP-Vi.[16] The slightly decreased solubility from BTMAP-Vi is attributed to the overall increased molecular size of Dex-Vi. Although hydroxyl groups tend to improve water solubility of organic compounds, it is believed the high charge density on Dex-Vi prevents the water solvent molecules from arranging into an ideal hydrogen-bonding orientation with the hydroxyl groups.[17] However, it is hypothesized that the solubility of the singly ($1e^-$) and doubly reduced ($2e^-$) states of Dex-Vi that have decreased positive charge density will benefit from the presence of these hydroxyl moieties and potentially possess higher solubilities than their BTMAP-Vi counterparts, although the isolation of these O_2-sensitive reduced viologen intermediates is challenging and thus was not attempted. Yet, this theory was partially supported through conducting a single-cycle two-electron reduction RFB experiment of Dex-Vi (Figure S4). At a high-concentration of 1.5 M, Dex-Vi demonstrated flowable behavior without the formation of precipitates in the doubly reduced state, whereas the two-electron reduction of BTMAP-Vi has only ever been reported in a RFB at a low concentration of 0.25 M presumably due to solubility issues of the doubly reduced state.[15] Equally important to solubility is the viscosity of the solution, which should be considered for practical application to optimize electrochemical charge transfer resistance and pumping cost. Viscosity data informs at which anolyte concentration flow and cell resistance will begin to sharply increase. The viscosity of Dex-Vi in pure water was measured to be 1.1 cP at 0.25 M, 1.8 cP at 0.50 M, 4.7 cP at 1.0 M, and 50 cP at 1.5 M (Figure S5). Although no data have been reported for BTMAP-Vi, the viscosity of viologens does not appear to be the limiting factor to the useable concentration. Instead, the solubility of the molecule, particularly in its singly and doubly reduced states, dictates the highest cycling concentration achievable without the formation of precipitates.

In addition to the advantageous physical properties of Dex-Vi over BTAMP-Vi, it is important to elucidate whether the additional hydroxyl moieties introduce substantial electrochemical perturbations to the redox behavior. We studied the fundamental electrochemical properties of Dex-Vi through a series of voltammetry and impedance measurements. Dex-Vi possesses a first electron formal potential (E_1^0) of -0.322 V vs. SHE and a second electron formal potential (E_2^0) of -0.699 V, which are slightly more positive than those of BTMAP-Vi of -0.349 V and -0.713 V (Figure 2A). The addition of hydroxyl groups has minimal effect on the redox potential as they are not directly involved in electron conjugation and only have minor electrostatic and entropic contributions to the redox energetics. In addition to the thermodynamics, the kinetics of the redox species were investigated through cyclic voltammetry (CV) with different scan rates and electrochemical impedance spectroscopy (EIS). A reduced state diffusion coefficient (D_1^R) of 1.9×10^{-6} $cm^2 \cdot s^{-1}$ for $[Dex\text{-}Vi]^{3+}$ and an oxidized state diffusion coefficient (D_1^O) 2.3×10^{-6} $cm^2 \cdot s^{-1}$ for $[Dex\text{-}Vi]^{4+}$ were determined at the first reduction peak (Figures 2B&C). This is comparable to the D_1^R and D_1^O values of 2.7×10^{-6} $cm^2 \cdot s^{-1}$ and 2.4×10^{-6} $cm^2 \cdot s^{-1}$ for $[BTMAP\text{-}Vi]^{3+}$ and $[BTMAP\text{-}Vi]^{4+}$, respectively (Figures S7 & S8). EIS data showed combined diffusion coefficients (D_1^{EIS}) of 3.9×10^{-6} $cm^2 \cdot s^{-1}$ and 4.1×10^{-6} $cm^2 \cdot s^{-1}$ and standard rate constants (k_1^0) of 5.0×10^{-2} $cm \cdot s^{-1}$ and 8.9×10^{-2} $cm \cdot s^{-1}$ for the first reductions of Dex-Vi and BTMAP-Vi, respectively (Figure 2D). The second electron diffusion coefficients (D_2^R, D_2^O, and D_2^{EIS}) and rate constants (k_2^0) of Dex-Vi are also of the same order of magnitude as those of BTMAP-Vi (Figures S9-S13). The facile electrochemical kinetics of Dex-Vi confirms that the hydroxyl groups should impose no significant diffusional or electron kinetic barriers that may increase the electrochemical resistance and diminish power output of the RFB through overpotential losses.

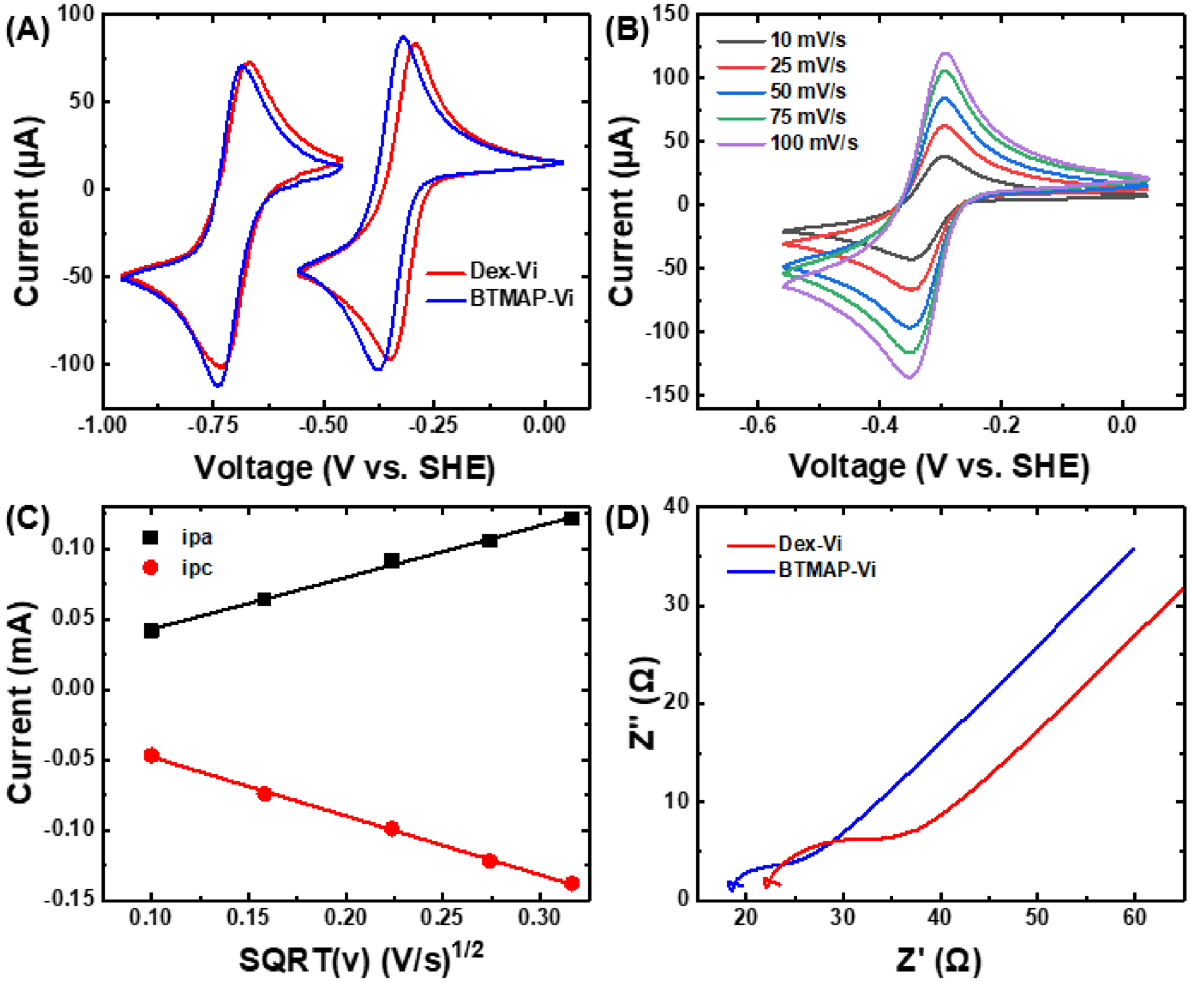

Figure 2. Cyclic voltammograms of (A) the first and second redox states of BTMAP-Vi (blue) and Dex-Vi (red) and (B) the first redox state of Dex-Vi at different scan rates. (C) Randles-Sevcik plot of the first redox state of Dex-Vi. (D) Experimental EIS spectra of BTMAP-Vi (blue) and Dex-Vi (red) measured at their E_1^0.

Permeability measurements reveal Dex-Vi is highly compatible with anion-exchange membranes with a permeance of $2.3\text{x}10^{-11}$ $cm^2 \cdot s^{-1}$ through Selemion DSV membrane, which is an order of magnitude lower than the reported value of $6.7\text{x}10^{-10}$ $cm^2 \cdot s^{-1}$ for BTMAP-Vi (Figure 3A and S14-S15).[18] There are two plausible reasons for this improved membrane exclusion. Firstly, Dex-Vi has an increased molecular size due to the presence of the hydroxy groups, slowing its diffusion through the membrane pores. Secondly, the hydroxy groups increase the water affinity of Dex-Vi, enlarging its Stokes radius, which lowers ion mobility, increases its desolvation energy, and inhibits entry into micro-pores. Thus, Dex-Vi should exhibit minimal crossover during RFB cycling.

In addition to the electrochemical kinetics and solution diffusional behavior, it is important to examine the lifetime of the organic redox species, which currently hinders the commercialization of AORFBs.[19] We investigated the chemical stability of the first redox processes of Dex-Vi using a symmetric, volumetrically-unbalanced flow cell inside an N_2 glovebox.[29] Dex-Vi exhibited no decay in a symmetric flow cell configuration over sixteen days (150 cycles) of continuous charge-discharge cycling (Figure 3C), which is slightly better than the reported minimal symmetric cell decay rate of BTMAP-Vi of 0.0016% per day under the same electrolyte conditions.[12,29,30] The improved symmetric cell stability of Dex-Vi may be due to its higher basicity tolerance, which may be of concern when imperfect oxygen exclusion inside the glovebox results in oxygen reduction at the anode (Figure S16) and HER at the negative electrode. This theory was partially supported through degradation kinetics experiments of Dex-Vi and BTMAP-Vi in sodium hydroxide. Dex-Vi was found to degrade in base in a first order mechanism with respect to Dex-Vi concentration and one-half order with respect to hydroxide concentration, resulting in a degradation rate constant k of $2.3\text{x}10^{-6}\ \text{s}^{-1}\cdot\text{M}^{-1/2}$ for the overall one-and-one-half order reaction (Figure 3B and S17-S19). Surprisingly, BTMAP-Vi exhibited an order of magnitude faster degradation rate in hydroxide than Dex-Vi with a k of $6.9\text{x}10^{-5}\ \text{s}^{-1}\cdot\text{M}^{-1/2}$ under identical conditions and assuming the same reaction order (Figure 3B and S20). Although these kinetic results match well with the improved Dex-Vi stability over BTMAP-Vi in symmetric cell cycling, further studies should be conducted to elucidate the role of the Dex-Vi alcohol moieties in this proposed degradation mechanism and to fully understand the origin of the hydroxide in the anolyte solution.

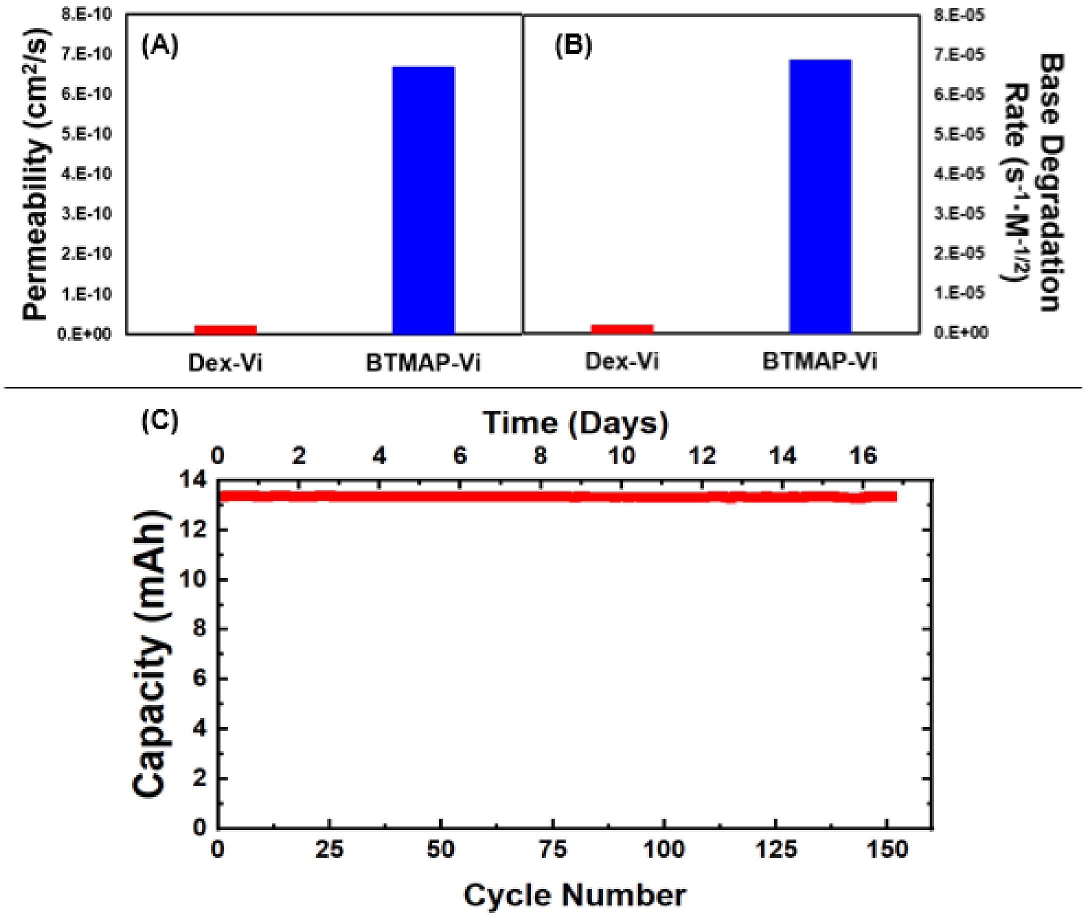

Figure 3. (A) Comparison of the permeabilities of Dex-Vi and BTMAP-Vi through DSV anion exchange membrane in H-cell. (B) Comparison of the apparent degradation rate constant of Dex-Vi and BTMAP-Vi in sodium hydroxide. The degradation rate was found to be first order with respect to viologen concentration and one-half order with respect to hydroxide concentration. (C) Symmetric cell cycling performance of 0.1 M Dex-Vi in 1 M NaCl with AMV membrane.

After confirming the superior properties of Dex-Vi, we conducted full RFB tests to evaluate the practical cycling performance of the Dex-Vi anolyte. For full cell experiments, Dex-Vi was paired with BTMAP-Fc, which is a stable catholyte also with low permeance.[12,31] Although a higher voltage catholyte such as TEMPO could be used to increase cell voltage and power, BTMAP-Fc was selected and used in excess to demonstrate the true stability of the Dex-Vi analyte as TEMPO and other Ferrocene derivatives (i.e., FcNCl) have crossover concerns that may interfere with the anolyte cycling performance. Pure Dex-Vi was cycled in RFBs to investigate its ideal performance and followed standard current rate variation behavior (Figure S21). A low-concentration (0.1 M) RFB cycling test of Dex-Vi in an anolyte-limiting configuration displayed no observable decay over two weeks of cycling (1,200+ cycles) (Figure 4A). High concentration cycling was also carried out in an anolyte-limiting configuration to demonstrate the high practical capacity of Dex-Vi. Dex-Vi still exhibited no discernable decay after one month of continual cycling at a concentration of 1.5 M (theoretical anolyte volumetric capacity of 40.2 Ah·L^{-1}), which is equal to the highest demonstrated concentration for any reported stable organic anolyte redox species in neutral aqueous solution (Figures 4B).[12,15–17,22] Post-cycling CV of the catholyte showed minimal Dex-Vi redox feature (Figure S23), confirming good membrane compatibility of Dex-Vi even at high concentration. The stable full cell performance signifies that there is no increase in chemical degradation with increased concentration and that crossover is miniscule as the Dex-Vi symmetric cell demonstrated a similar decay rate. The decay rate of BTMAP-Vi was reported to be 36.5% per year (0.1% per day) when it was utilized at 1.3 M in an anolyte-limiting cell with BTMAP-Fc catholyte and DSV membrane.[18] Thus, Dex-Vi displays drastically improved capacity retention compared to BTAMP-Vi even at a higher concentration in an anolyte-limiting configuration with the same catholyte and membrane. We attribute the drastically increased capacity retention of Dex-Vi to both its enhanced chemical stability and improved membrane compatibility (Figure 3A and 3B).

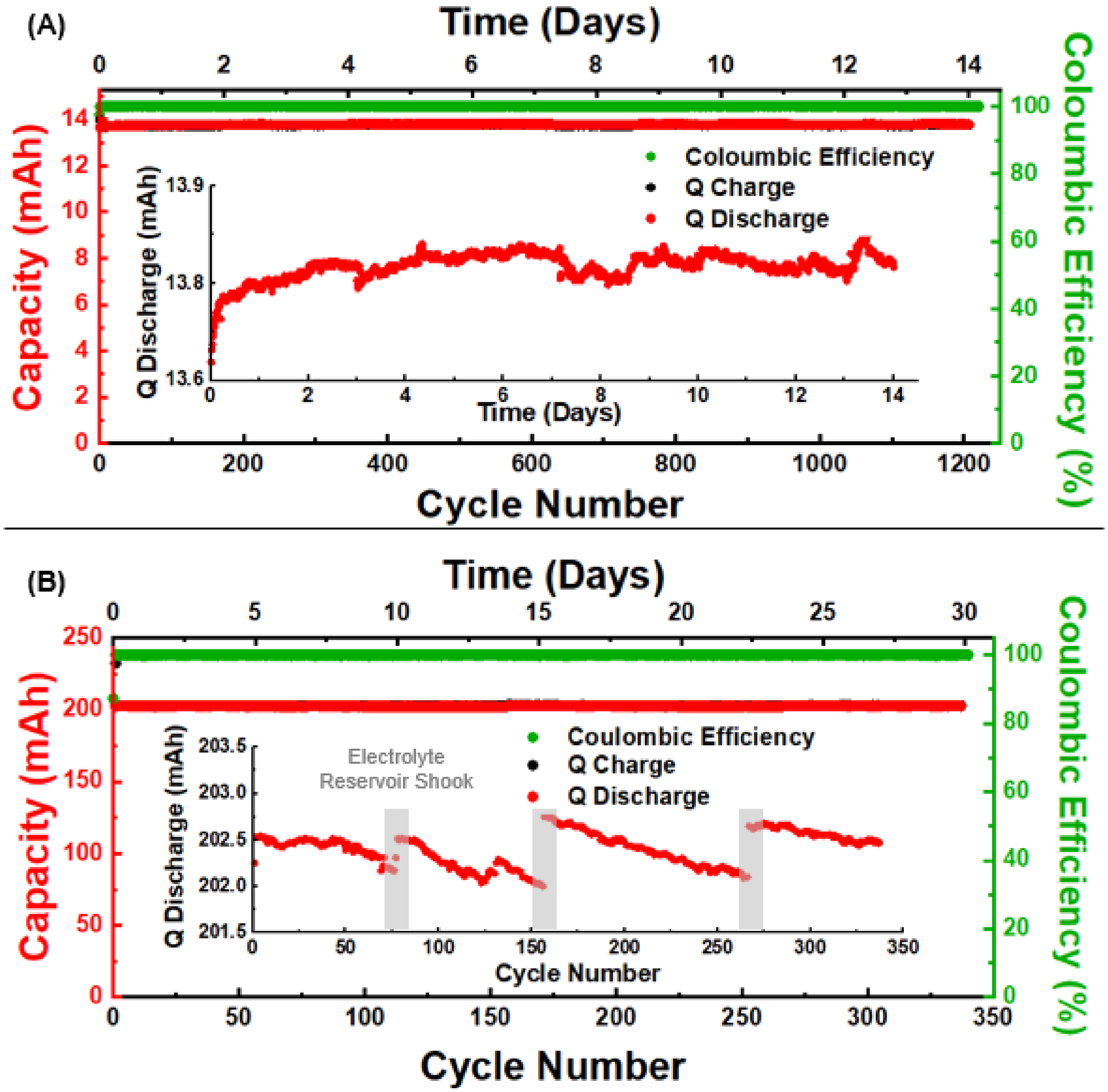

Figure 4. (A) Full cell cycling performance of 0.1 M Dex-Vi in 1 M NaCl with volumetric excess of 0.75 M BTAMP-Fc catholyte and DSV membrane. (B) Full cell cycling performance of 1.5 M Dex-Vi (40.2 Ah·L^{-1}) in pure water with volumetric excess of 0.75 M BTAMP-Fc catholyte and DSV membrane. The slight capacity increase areas (marked in grey) correspond to recovered electrolyte stuck on the wall of electrolyte reservoirs upon shaking the reservoirs.

Discussion

Simple cost analysis (see Supplemental Information for details) reveals that Dex-Vi was synthesized at a raw material cost of \$6.8/Ah (\$0.30/g) on a lab-scale whereas commercially available BTMAP-Vi is \$1089/Ah (\$54.4/g) for a small-batch (TCI Chemicals) when considering the species as one-electron anolytes. The lab-scale raw materials cost of BTMAP-Vi was estimated to be \$23/Ah (\$1.1/g). The significant difference between estimated BTMAP-Vi raw material cost and commercial cost can be partially attributed to the additional labor and materials costs associated with the intensive ion-exchange procedures, which are not required for Dex-Vi. Although data was not readily available to estimate the mass production (100,000+ Metric Ton) cost of Dex-Vi, the cost of 1 Metric Ton was estimated to be \$39/kg. This is unprecedented considering that 2,6-dihydroxy anthraquinone (DHAQ), another promising aqueous anolyte, has a small-batch cost of \$113/Ah (\$15/g), an estimated cost of \$300/kg at the 1 Metric Ton scale, and a mass production cost of \$3/kg (\$23/kAh) as a two-electron anolyte.[32] If Dex-Vi follows a similar cost-reduction trend to anthraquinone, the mass production cost would be 39¢/kg (\$8.7/kAh). Furthermore, anthraquinones require additional costly functionalization for increased membrane compatibility, aqueous solubility, and chemical stability and also require highly basic solution (pH > 12) to achieve ideal performance, making it difficult to develop a base-stable catholyte with similar volumetric capacity to pair with in practical RFBs.[33–36] In contrast, Dex-Vi can be readily paired with existing TEMPO and Ferrocene catholytes to enable higher voltage AORFBs with uncompromised volumetric capacity.[16,31,37]

Table 1. Summary of the parameter comparison between BTMAP-Vi and Dex-Vi. *No aqueous anolyte-limiting RFB data is available for MV, and yearly decay was extrapolated based on available MV symmetric cell data which does not account for additional decay due to crossover.

Anolyte	RFB Viologen Molarity ($1e^-$)	DSV Membrane Permeability (cm^2/s)	E_1^0 / E_2^0 (V vs. SHE)	k_1^0 (cm/s)	Anolyte-limiting RFB Stability (% decay/year)	Small-batch Cost (\$/Ah)
MV [23,24]	0.5	3.4×10^{-9}	-0.450 / NA	2.8×10^{-4}	>547.5%*	\$419
BTMAP-Vi [18,15]	1.5	6.7×10^{-10}	-0.349 / -0.713	8.9×10^{-2}	36.5%	\$1,089
Dex-Vi	1.5	2.3×10^{-11}	-0.322 / -0.699	5.0×10^{-2}	~0%	\$6.8

Conclusion

This work presents a simple synthetic route for preparing a rationally designed viologen derivative, Dex-Vi. The hydroxyl moieties of Dex-Vi have minimal effect on redox potential and electrochemical kinetics while offering superior membrane compatibility and chemical stability as compared to BTMAP-Vi. Moreover, we have demonstrated drastically improved cycling stability of Dex-Vi at high concentration as compared to BTMAP-Vi. In light of the extremely low cost and high performance of Dex-Vi, it can serve as a new benchmark aqueous anolyte to pair with anion-exchange membranes in neutral pH RFBs and paves the way for the further development of commercially viable neutral pH AORFBs at grid-scale.

Experimental

Synthesis of Dextrosil Viologen

4,4-dipydridyl and 3-chloro-2-hydroxypropyl trimethylammonium chloride were obtained from Oakridge Chemical and Tokyo Chemical Industry Co., respectively, and used without further purification. Firstly, 12 g (0.077 mol) of 4,4-dipyridyl was added to 60 mL (0.22 mol) of 3-chloro-2-hydroxypropyl trimethylammonium chloride (65 wt% in water) in an autoclave reactor. The solution was then transferred to a stainless-steel autoclave with PTFE liner (100 mL) and heated to 120 ^{o}C for 24 hr. After the reaction, ethanol and then acetone were added to the resultant aqueous solution in sequential order in a 1:9:10 (product:ethanol:acetone) volume ratio to precipitate out the pure product. The off-white product was filtered, washed with acetone, and vacuum dried. A high overall yield of 71% (33 g) was obtained.

Structure Characterization

A Bruker Avance-400 NMR spectrometer was used to conduct ^{1}H-NMR experiment, which was analyzed using the Bruker TopSpin software. Dex-Vi: ^{1}H NMR (D_2O δ 4.80, 400 MHz): δ 3.30 (s, 9H), 3.71 (quint, 4H), 4.69 (q, 2H), 4.86 (q, 2H), 5.03 (d, 2H) (Fig. S3). Single crystal data was obtained using a Bruker Quazar APEX2 with a Mo Kα IμS radiation source.

Solubility

A measured amount of Dex-Vi was partially dissolved in pure water. The solution was then centrifuged. The supernatant was decanted, and the volume was measured. The remainder of the solid was dried in a vacuum oven and weighed. Finally, the weight of remaining Dex-Vi was subtracted from the initial added mass to obtain the amount dissolved in the supernatant, permitting calculation of the maximum soluble concentration. The solubility tests were performed at room temperature of 18 ^{o}C.

Viscosity

Viscosity measurements were carried out using an Ares G2 rheometer (TA Instruments) with an advanced Peltier system at 25 ^{o}C.

Permeability

0.33 M Dex-Vi in pure water was separated by an anion-exchange membrane (DSV) from 1 M NaCl in an H-cell. These concentrations were chosen through empirically trial-and-error and showed little osmotic pressure driven water transport through the membrane to balance ion-strength. The cell was agitated on a shaker to partially simulate flow dynamics. Aliquots of the receiving end (1 M NaCl side) where taken every few days, and the removed volume was replaced with 1 M NaCl. The concentration of Dex-Vi in the aliquot was determined by measuring the absorbance at 285 nm using a UV-Vis spectrophotometer. The concentration as a function of time data was then used to calculate the permeability constant of Dex-Vi.[38]

Electrochemical Measurements

Cyclic Voltammetry (CV) and Electrochemical Impedance Spectroscopy (EIS) experiments were ran using a PalmSens4 potentiostat with the PSTrace software. Electrochemical experiments were performed in 1.0 M NaCl supporting electrolyte using 15 mM of active material at room temperature (18 ^oC). Formal potentials for the redox couples were estimated by taking the average potential between the cathodic and anodic peak. Diffusional behavior was investigated by varying the scan rate between 10-100 $mV \cdot s^{-1}$ for the first electron reduction and 50-200 $mV \cdot s^{-1}$ for the second electron reduction, and the diffusion constants of the reduced and oxidized states (D^R and D^O) were determined via the Randles-Sevcik equation assuming ideal reversible behavior. Potentiostatic EIS measurements were used for determination of a combined diffusional constant of the reduced and oxidized states (D^{EIS}) and of the standard electron kinetic rate constant (k^o). These EIS measurements were performed at the formal reduction potential (held for 30 seconds before measurement) in which the concentration of the two redox states at the electrode surface are assumed to be the same and equal to half of the initially prepared redox species concentration.

Flow Cell Cycling Measurements

The RFB measurements were carried out in a custom-made zero-gap device previously reported by Li et al.[39,40] Both symmetric cell and full cell measurements were conducted using a Bio-Logic VSP-300 potentiostat or a Neware BTS4000 battery tester at room temperature (~20 ^oC). In symmetric cell, 0.1 M of Dex-Vi in 1 M NaCl (pre-charged to 50% SOC of the first electron reduction using FcNCl as the counter cathode in bulk electrolysis) was utilized on both sides with the capacity limiting side (CLS) consisting of 5 mL of solution and the non-capacity limiting side (NCLS) consisting of 10 mL of solution separated by a Selemion AMV anion-exchange membrane (Asahi Glass Co.). Rate performance was investigated using 5 mL 0.1 M Dex-Vi anolyte and 5 mL 0.2 M BTMAP-Fc catholyte both in 1 M NaCl with DSV anion-exchange membrane. The low concentration experiment was performed using 5.5 mL of 0.1 M Dex-Vi anolyte in 1 M NaCl, 10 mL 0.1 M BTMAP-Fc, and a Selemion DSV anion-exchange membrane (Asahi Glass Co.) anion-exchange membrane. The high concentration Dex-Vi RFB full cell cycling was performed using 5 mL of 1.5 M Dex-Vi as the anolyte and 15 mL 0.75 M BTMAP-Fc as the catholyte, both of which were prepared in pure water without any supporting salt, with a DSV anion-exchange membrane.

Acknowledgements:

D.F. acknowledges the start-up funds from the University of Wisconsin-Madison. P.S. thank the support by Vice Chancellor for Research and Graduate Education (VCRGE) via 1975XX-135-AAI2755. S.J., W.L., and H.C.F. thank the support by the King Abdullah University of Science and Technology (KAUST) Office of Sponsored Research (OSR) under award no. OSR-2017-CRG6-3453.02. The authors would like to thank Prof. P. Gopalan for assistance with UV-Vis measurement, Prof. S. Stahl for the access to the N_2 glovebox, I. Guzei for assistance with data collection of single crystal X-ray diffraction, Zhiao Yu (Stanford University) for viscosity measurement. The Bruker Quazar APEX2 was purchased by UW–Madison Department of Chemistry with a portion of a generous gift from Paul J. and Margaret M. Bender.

References:

1. MINING.COM - Answering Mining’s Big Questions https://www.mining.com/.
2. Sánchez-Díez, E., Ventosa, E., Guarnieri, M., Trovò, A., Flox, C., Marcilla, R., Soavi, F.,

Mazur, P., Aranzabe, E., and Ferret, R. (2021). Redox flow batteries: Status and perspective towards sustainable stationary energy storage. J. Power Sources *481*, 228804.

3. Zhong, F., Yang, M., Ding, M., and Jia, C. (2020). Organic Electroactive Molecule-Based Electrolytes for Redox Flow Batteries: Status and Challenges of Molecular Design. Front. Chem. *8*, 451.
4. Li, Z., and Lu, Y.C. (2020). Material Design of Aqueous Redox Flow Batteries: Fundamental Challenges and Mitigation Strategies. Adv. Mater. *32*, 2002132.
5. Kwabi, D.G., Ji, Y., and Aziz, M.J. (2020). Electrolyte Lifetime in Aqueous Organic Redox Flow Batteries: A Critical Review. Chem. Rev. *120*, 6467–6489.
6. Singh, V., Kim, S., Kang, J., and Byon, H.R. (2019). Aqueous organic redox flow batteries. Nano Res. *12*, 1988–2001.
7. Luo, J., Hu, B., Hu, M., Zhao, Y., and Liu, T.L. (2019). Status and Prospects of Organic Redox Flow Batteries toward Sustainable Energy Storage. ACS Energy Lett. *4*, 2220–2240.
8. Ding, Y., Zhang, C., Zhang, L., Zhou, Y., and Yu, G. (2018). Molecular engineering of organic electroactive materials for redox flow batteries. Chem. Soc. Rev. *47*, 69–103.
9. Chen, H., Cong, G., and Lu, Y.C. (2018). Recent progress in organic redox flow batteries: Active materials, electrolytes and membranes. J. Energy Chem. *27*, 1304–1325.
10. Wei, X., Pan, W., Duan, W., Hollas, A., Yang, Z., Li, B., Nie, Z., Liu, J., Reed, D., Wang, W., et al. (2017). Materials and Systems for Organic Redox Flow Batteries: Status and Challenges. ACS Energy Lett. *2*, 2187–2204.
11. Winsberg, J., Hagemann, T., Janoschka, T., Hager, M.D., and Schubert, U.S. (2017). Redox-Flow Batteries: From Metals to Organic Redox-Active Materials. Angew. Chemie - Int. Ed. *56*, 686–711.
12. Beh, E.S., De Porcellinis, D., Gracia, R.L., Xia, K.T., Gordon, R.G., and Aziz, M.J. (2017). A neutral pH aqueous organic- organometallic redox flow battery with extremely high capacity retention. ACS Energy Lett. *2*, 639–644.
13. Li, W., Zheng, J., Hu, B., Fu, H.C., Hu, M., Veyssal, A., Zhao, Y., He, J.H., Liu, T.L., Ho-Baillie, A., et al. (2020). High-performance solar flow battery powered by a perovskite/silicon tandem solar cell. Nat. Mater. *19*, 1326–1331.
14. Li, W., Kerr, E., Goulet, M., Fu, H., Zhao, Y., Yang, Y., Veyssal, A., He, J., Gordon, R.G., Aziz, M.J., et al. (2019). A Long Lifetime Aqueous Organic Solar Flow Battery. Adv. Energy Mater. *9*, 1900918.
15. DeBruler, C., Hu, B., Moss, J., Liu, X., Luo, J., Sun, Y., and Liu, T.L. (2017). Designer Two-Electron Storage Viologen Anolyte Materials for Neutral Aqueous Organic Redox Flow Batteries. Chem *3*, 961–978.
16. Liu, Y., Goulet, M.A., Tong, L., Liu, Y., Ji, Y., Wu, L., Gordon, R.G., Aziz, M.J., Yang, Z., and Xu, T. (2019). A Long-Lifetime All-Organic Aqueous Flow Battery Utilizing

TMAP-TEMPO Radical. Chem *5*, 1861–1870.

17. Liu, Y., Li, Y., Zuo, P., Chen, Q., Tang, G., Sun, P., Yang, Z., and Xu, T. (2020). Screening Viologen Derivatives for Neutral Aqueous Organic Redox Flow Batteries. ChemSusChem *13*, 2245–2249.

18. Weber, A.Z., Mench, M.M., Meyers, J.P., Ross, P.N., Gostick, J.T., and Liu, Q. (2011). Redox flow batteries: A review. J. Appl. Electrochem. *41*, 1137–1164.

19. Brushett, F.R., Aziz, M.J., and Rodby, K.E. (2020). On Lifetime and Cost of Redox-Active Organics for Aqueous Flow Batteries. ACS Energy Lett. *5*, 879–884.

20. Dmello, R., Milshtein, J.D., Brushett, F.R., and Smith, K.C. (2016). Cost-driven materials selection criteria for redox flow battery electrolytes. J. Power Sources *330*, 261–272.

21. (3-Chloro-2-hydroxypropyl)trimethylammonium chloride | C6H15NOCl2 - PubChem https://pubchem.ncbi.nlm.nih.gov/compound/Dextrosil.

22. Hu, B., Tang, Y., Luo, J., Grove, G., Guo, Y., and Liu, T.L. (2018). Improved radical stability of viologen anolytes in aqueous organic redox flow batteries. Chem. Commun. *54*, 6871–6874.

23. Hu, B., Debruler, C., Rhodes, Z., and Liu, T.L. (2017). Long-Cycling aqueous organic Redox flow battery (AORFB) toward sustainable and safe energy storage. J. Am. Chem. Soc. *139*, 1207–1214.

24. Liu, T., Wei, X., Nie, Z., Sprenkle, V., and Wang, W. (2016). A Total Organic Aqueous Redox Flow Battery Employing a Low Cost and Sustainable Methyl Viologen Anolyte and 4-HO-TEMPO Catholyte. Adv. Energy Mater. *6*.

25. Jin, S., Fell, E.M., Vina-Lopez, L., Jing, Y., Michalak, P.W., Gordon, R.G., and Aziz, M.J. (2020). Near Neutral pH Redox Flow Battery with Low Permeability and Long-Lifetime Phosphonated Viologen Active Species. Adv. Energy Mater. *10*.

26. Debruler, C., Hu, B., Moss, J., Luo, J., and Liu, T.L. (2018). A Sulfonate-Functionalized Viologen Enabling Neutral Cation Exchange, Aqueous Organic Redox Flow Batteries toward Renewable Energy Storage. ACS Energy Lett. *3*, 663–668.

27. EU RISK ASSESSMENT-(3-CHLORO-2-HYDROXYPROPYL)TRIMETHYLAMMONIUM CHLORIDE European Union Risk Assessment Report (3-CHLORO-2-HYDROXYPROPYL)TRIMETHYLAMMONIUM CHLORIDE (CHPTAC) RISK ASSESSMENT FINAL APPROVED VERSION.

28. Rabenau, A. (1985). The Role of Hydrothermal Synthesis in Preparative Chemistry. Angew. Chemie Int. Ed. English *24*, 1026–1040.

29. Goulet, M.-A., and Aziz, M.J. (2018). Flow Battery Molecular Reactant Stability Determined by Symmetric Cell Cycling Methods. J. Electrochem. Soc. *165*, A1466–A1477.

30. Robb, B.H., Waters, S.E., and Marshak, M.P. (2020). Minimizing Oxygen Permeation in Metal-Chelate Flow Batteries. ECS Trans. *97*, 237–245.

31. Chen, Q., Li, Y., Liu, Y., Sun, P., Yang, Z., and Xu, T. (2021). Designer Ferrocene Catholyte for Aqueous Organic Flow Batteries. ChemSusChem *14*, 1295–1301.

32. Yang, Z., Tong, L., Tabor, D.P., Beh, E.S., Goulet, M.A., De Porcellinis, D., Aspuru-Guzik, A., Gordon, R.G., and Aziz, M.J. (2017). Alkaline Benzoquinone Aqueous Flow Battery for Large-Scale Storage of Electrical Energy. Adv. Energy Mater. *8*.

33. Wu, M., Jing, Y., Wong, A.A., Fell, E.M., Jin, S., Tang, Z., Gordon, R.G., and Aziz, M.J. (2020). Extremely Stable Anthraquinone Negolytes Synthesized from Common Precursors. Chem *6*, 1432–1442.

34. Ji, Y., Goulet, M.A., Pollack, D.A., Kwabi, D.G., Jin, S., De Porcellinis, D., Kerr, E.F., Gordon, R.G., and Aziz, M.J. (2019). A Phosphonate-Functionalized Quinone Redox Flow Battery at Near-Neutral pH with Record Capacity Retention Rate. Adv. Energy Mater. *9*.

35. Jin, S., Jing, Y., Kwabi, D.G., Ji, Y., Tong, L., De Porcellinis, D., Goulet, M.A., Pollack, D.A., Gordon, R.G., and Aziz, M.J. (2019). A Water-Miscible Quinone Flow Battery with High Volumetric Capacity and Energy Density. ACS Energy Lett. *4*, 1342–1348.

36. Gerhardt, M.R., Tong, L., Gómez-Bombarelli, R., Chen, Q., Marshak, M.P., Galvin, C.J., Aspuru-Guzik, A., Gordon, R.G., and Aziz, M.J. (2017). Anthraquinone Derivatives in Aqueous Flow Batteries. Adv. Energy Mater. *7*.

37. Zhou, W., Liu, W., Qin, M., Chen, Z., Xu, J., Cao, J., and Li, J. (2020). Fundamental properties of TEMPO-based catholytes for aqueous redox flow batteries: effects of substituent groups and electrolytes on electrochemical properties, solubilities and battery performance. RSC Adv. *10*, 21839–21844.

38. Kwabi, D.G., Lin, K., Ji, Y., Kerr, E.F., Goulet, M.A., De Porcellinis, D., Tabor, D.P., Pollack, D.A., Aspuru-Guzik, A., Gordon, R.G., et al. (2018). Alkaline Quinone Flow Battery with Long Lifetime at pH 12. Joule *2*, 1894–1906.

39. Li, W., Fu, H.C., Zhao, Y., He, J.H., and Jin, S. (2018). 14.1% Efficient Monolithically Integrated Solar Flow Battery. Chem *4*, 2644–2657.

40. Li, W., Kerr, E., Goulet, M.A., Fu, H.C., Zhao, Y., Yang, Y., Veyssal, A., He, J.H., Gordon, R.G., Aziz, M.J., et al. (2019). A Long Lifetime Aqueous Organic Solar Flow Battery. Adv. Energy Mater. *9*, 1900918.